

Macroscopic Chirality of Twist-Bent Nematic Phase in Bent Dimers Confirmed by Circular Dichroism

Warren D. Stevenson^a, Xiangbing Zeng^{*a}, Chris Welch^b, Anil K. Thakur^a, Goran Ungar^{*a,c}
and Georg H. Mehl^b

^aDepartment of Materials Science and Engineering, University of Sheffield, Sheffield S1
3JD, UK

^bDepartment of Chemistry, University of Hull, Hull HU6 7RX, UK

^cState Key Laboratory for Mechanical Behavior of Materials, School of Material Science and
Engineering, Xian Jiaotong University, Xi'an 710049, P.R. China

Supplementary Information

Contents

1.0 – Materials	1
2.0 – Conoscopy	2
3.0 – GIXS Patterns of CBC9CB	3
3.1 – GIXS Spacings	3
4.0 – UV-Vis Spectra & Cell Gap Determination	4
5.0 – CD and Ellipticity	5
5.1 – Additional CD Data	5
5.2 – CD in Other Sample Positions	6
5.3 – CD of non-homeotropically oriented N _{tb} phase	7

1.0 – Materials

Full synthetic details for the synthesis of the materials and of the full chemical characterisation have been reported for the series of CBC_nCB materials recently in [1] and for the set of the DTC5C_n materials in [2].

[1] K. Krzyżewska, T. Jaroch, A. Maranda-Niedbała, D. Pociecha, E. Górecka, Z. Ahmed, C. Welch, G. H Mehl, A. Proń, R. Nowakowski, Supramolecular organization of liquid-crystal dimers - bis-cyanobiphenyl alkanes on HOPG by scanning tunneling microscopy, *Nanoscale*, 2018; 10,16201-16210, DOI: 10.1039/C8NR02069H.

[2] W. D. Stevenson, H.X. Zou, X. B. Zeng, C. Welch, G. Ungar, G. H. Mehl, Dynamic Calorimetry and XRD Studies of the Nematic and Twist-Bend Nematic Phase Transitions in a Series of Dimers with Increasing Spacer Length, *PCCP*, 2018, **20**, 25268 – 25274; DOI [10.1039/C8CP05744C](https://doi.org/10.1039/C8CP05744C).

2.0 – Conoscopy

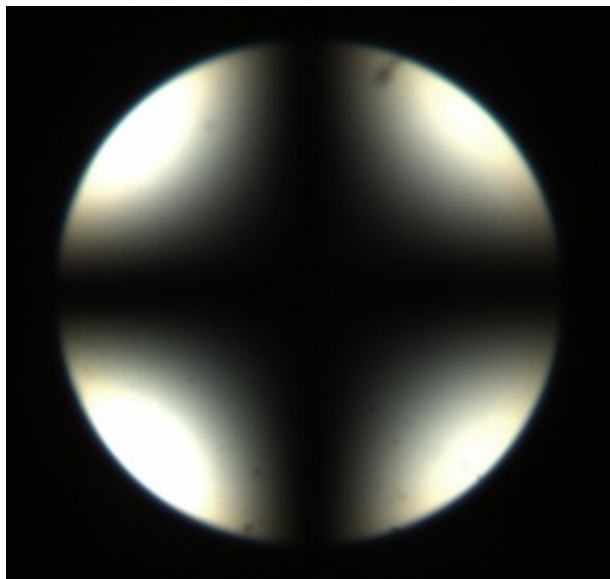


Figure S1. Conoscopic image of the N_{tb} phase in homeotropic alignment after shearing, DTC5C9 at 100°C.

3.0 – GIXS Patterns of CBC9CB

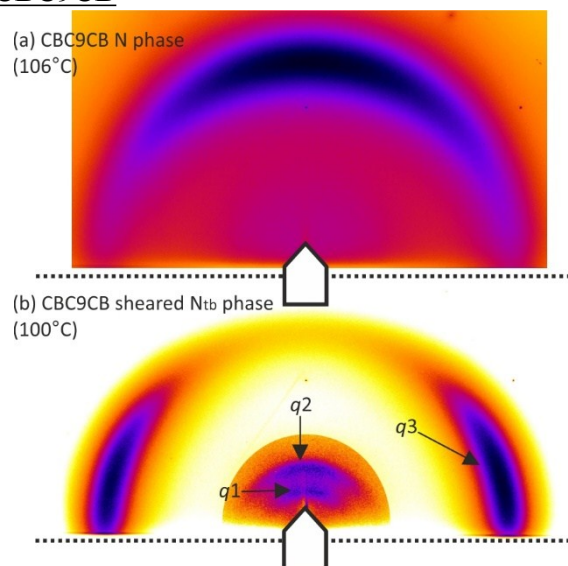


Figure S2. Representative GIXS patterns of CBC9CB. q_1 -3 denote the scattered wave vectors corresponding to the scattering peaks. (a) N phase, un-sheared showing mostly planar orientation. (b) Homeotropic N_x phase after shearing at 100°C. In (b) the WAXS intensity (q_3) has been increased by a factor of 4 compared to the SAXS for display purposes.

3.1 – GIXS Spacings

Table S1 contains the measured spacings of the broad scattering peaks found in the GIXS pattern of each sample of both nematic phases.

Table S1 – DTC5Cn SAXS and WAXS spacings

n	N Phase			N_{tb} Phase		
	d_1 (nm)	d_2 (nm)	d_3 (nm)	d_1 (nm)	d_2 (nm)	d_3 (nm)
5	3.9	1.8	0.50	3.8	1.8	0.49
7	4.0	1.9	0.51	4.0	1.9	0.51
9	4.5	2.1	0.51	4.3	2.0	0.50

$d_{(1,2)}=2\pi/q_{(1,2)}$, $d_3=1.117(2\pi/q_3)^{4/3}$. For diffuse SAXS peaks Bragg's law does not strictly apply, meaning $d_{1,2}$ are slight underestimates of the real spacings.

4.0 – UV-Vis Spectra & Cell Gap Determination

The cell gaps of the sheared CD samples were estimated by absorption calibration. A second set of cells were created, but with a polymer spacer layer separating the quartz glass plates at a fixed distance (Figure S3a). The thickness of the spacer layer (T_s) was found for each sample using a Bruker Contour Elite microscope (Figure S3b and Table S2). The spacer thickness was found to vary over the surface of each sample, as well as between samples, and so an average T_s (3.4 μm) was calculated and used as a constant for all six samples. The absorption spectra of the spacer samples were measured in the N_{tb} phase after shearing. The spacer made shearing more difficult and less effective, which is why spacers were not used for CD measurements in the first instance. The absorption spectra of the spacer cells were then averaged to produce a reference absorption curve (black in Figure S3c). The cell gaps (G) of the original CD samples were then estimated using the average T_s and the factor between sample absorbance and the reference curve. For example, in DTC5C7: $G = (2.2/2.1) * 3.4 \mu\text{m} = 3.6 \mu\text{m}$. The CD data shown in the main text and in section 3.0 were normalized using the G value of the corresponding sample.

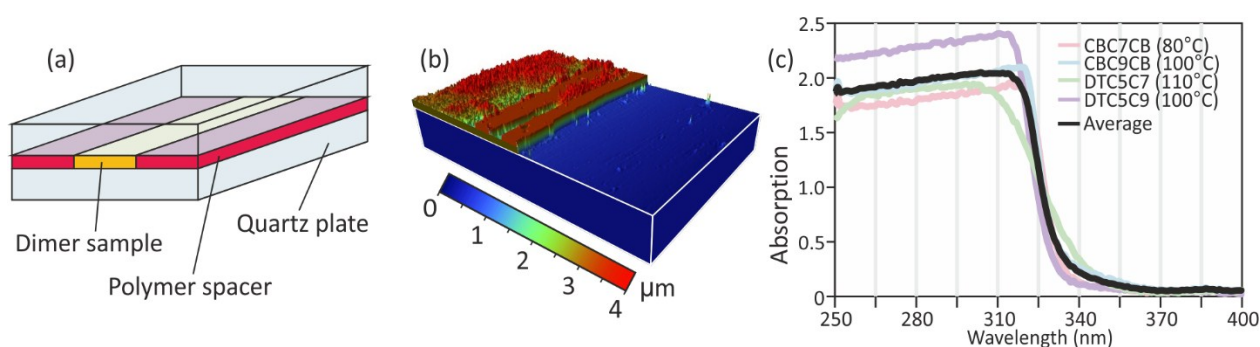


Figure S3 – (a) Diagram of a quartz sandwich cell with a spacer layer (red). (b) Example 3D contour image of a $1.3 \times 1 \mu\text{m}$ region of an empty cell (without the top plate on), showing the spacer wall height (red) relative the surface of the bottom glass plate (blue). (c) UV-Vis absorption spectra of studied dimers. Black is the average/absorption reference curve.

Table S2 – Estimation of Sample Cell Gap

Sample	λ (nm)	$A(\lambda)$	$A_{ref}(\lambda)$	T_s (μm)	G (μm)
DTC5C5	300	2.3	2.1	*	3.7
DTC5C7	301	2.2	2.1	2.8	3.6
DTC5C9	296	2.0	2.0	3.6	3.4
CBC7CB	300	1.8	2.1	3.3	2.9
CBC9CB	300	1.8	2.1	3.9	2.9
			T_s Avg =	3.4	

*A DTC5C5 spacer cell was not created due to insufficient supply. λ = wavelength, $A(\lambda)$ is the sample absorption at a given wavelength, $A_{ref}(\lambda)$ is the reference absorption at the same wavelength, T_s is the measured spacer thickness and G = estimated cell gap of the original sample set discussed in the main text and in section 3.0.

5.0 – CD and Ellipticity

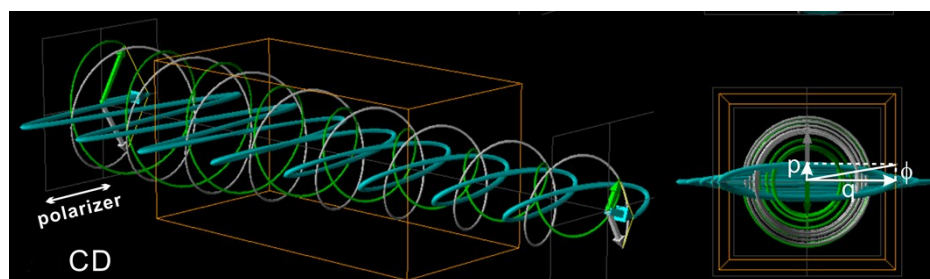


Figure S4. Electric field wave representation of the conversion of linearly polarized to elliptically polarized light on passage through a circularly dichroic medium. Linearly polarized light enters from the left, and is split into left and right circularly polarized components, with the extinction coefficients of the two in the ratio 2:1. The view along the light path is shown on the right. The ellipticity $\phi = \arctan(p/q)$. Note that the ellipticity in a typical CD experiment is very much smaller than that shown. Emanim, written by Andras Szilagy and available from <https://emanim.szilab.org/> was used for producing the figure.

5.1 – Additional CD Data

Figure S5 contains CD data of the N_{tb} phase and N phase for samples not shown in the main text. N_{tb} spectra were recorded directly after the shearing process using the method and instrumentation described in the main text.

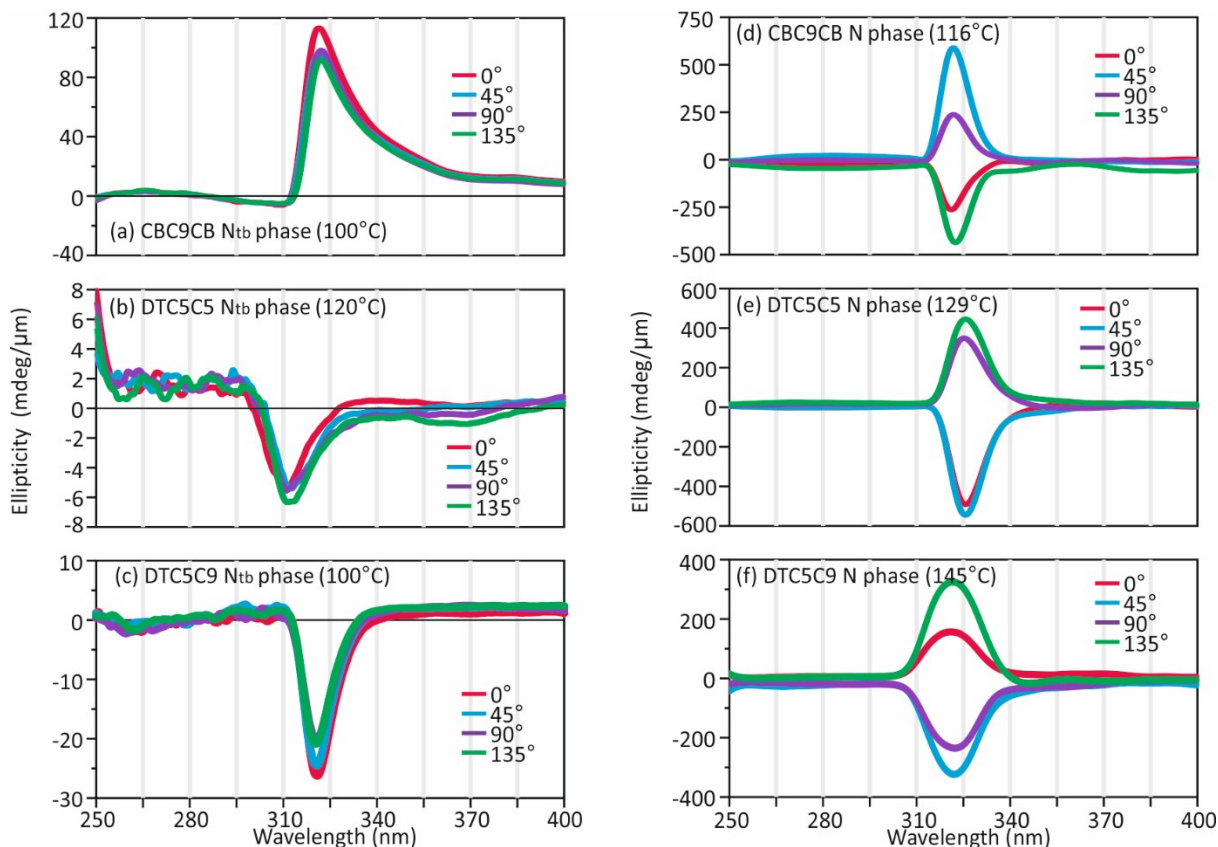


Figure S5 – Additional CD data of the N_{tb} phase (at T_{shear}) (a)-(c) and N phase (d)-(f).

5.2 – CD in Other Sample Positions

The CD of each sample was investigated in at least 3 different positions (one of which is shown above or in the main text). The sample position was changed simply by translating the sheared sandwich cell along the heated stage while in the N_{tb} phase. The CD spectra were also measured after quickly flipping the cell over on the hot stage. Representative spectra of CBC7CB and DTC5C7 are shown below in Figure S3. Peaks vary more on rotation in CBC7CB because the homeotropic alignment contained more defects than in DTC5C7.

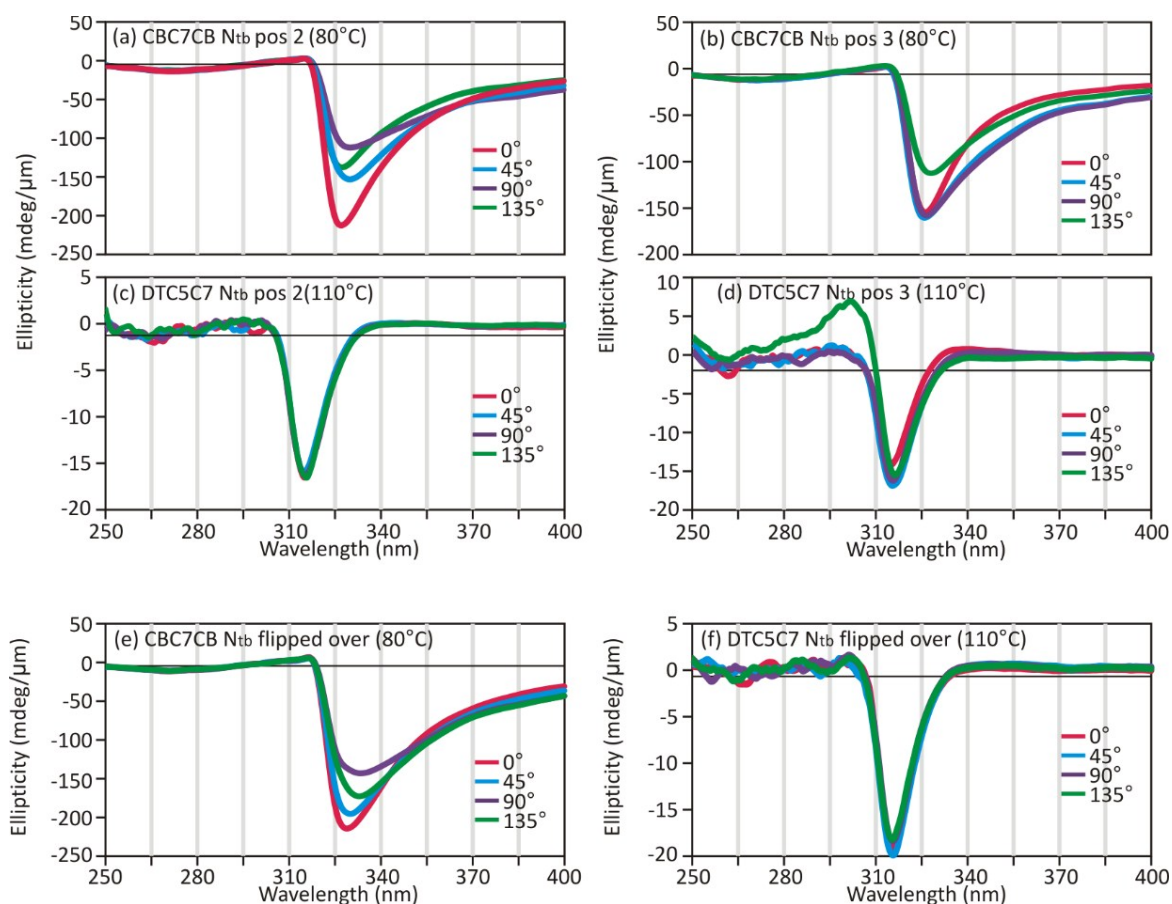


Figure S6 – Sheared N_{tb} phase of CBC7CB in position 2(a) and 3(b). Sheared N_{tb} phase of DTC5C7 in position 2(c) and 3(d). Flipped cell containing CBC7CB(e) and DTC5C7(f).

5.3 – CD of non-homeotropically oriented N_{tb} phase

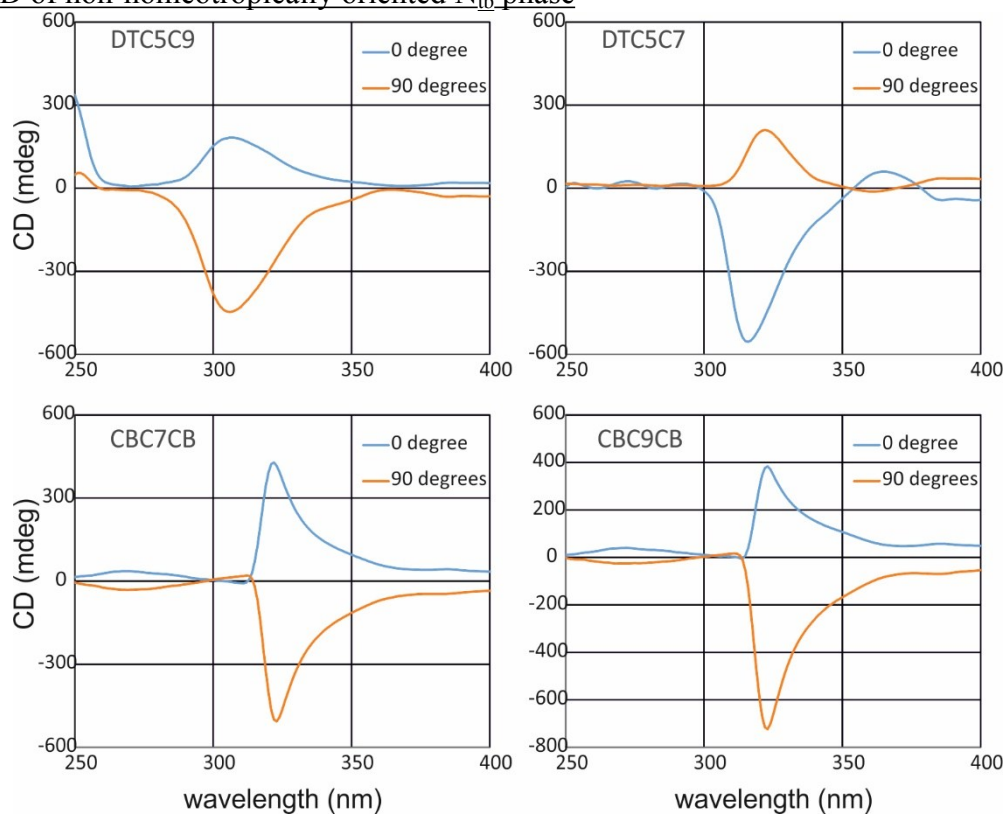


Figure S7. Example CD spectra of compounds in the N_{tb} phase but not homeotropically aligned, changes dramatically when samples are rotated by 90° along the light beam direction.